

SPIN-DOWN OF RAPIDLY ROTATING NEUTRON STARS

LEE SAMUEL FINN¹ AND STUART L. SHAPIRO²

Center for Radiophysics and Space Research, Cornell University

Received 1989 October 16; accepted 1990 February 22

ABSTRACT

As the angular momentum of a neutron star changes, as a result of electromagnetic or gravitational radiation or of accretion, its period changes. For slowly rotating pulsars, the moment of inertia is constant and the period changes linearly with the angular momentum. For rapidly rotating pulsars, however, the star's oblateness, and hence its moment of inertia, changes appreciably as the period evolves, with important observational consequences. Here we examine how the oblateness of a spinning neutron star affects the evolution of its period. Modeling an evolving pulsar as a sequence of homogeneous, uniformly rotating Newtonian Maclaurin spheroids, we determine how the period P , the period time derivative \dot{P} , and the braking index n_B vary with time as a result of dissipation via electromagnetic radiation, gravitational radiation, or a combination of the two. We also examine how these observable parameters vary with steady accretion. We consider two evolutionary equilibrium sequences: incompressible and compressible. In the first the density is constant, while in the second it is controlled by a polytropic equation of state. We find that it is possible (and by no means unlikely) that during the early evolution of a rapidly rotating star the rotational frequency may increase even as the angular momentum decreases. This behavior depends critically on the adopted nuclear equation of state.

As illustrative applications, we analyze the Crab pulsar spin evolution from birth to the present time, and the future evolution of a very rapidly rotating pulsar with an initial period of 0.5 ms. We point out that a modest fractional triaxial deformation of $\sim 5 \times 10^{-7}$ in such a rapidly spinning neutron star can generate a gravitational radiation amplitude of $\sim 2 \times 10^{-25}$ at the Earth, which is detectable using present-day bar detector technology, tuned to the correct frequency. We also show that eventual collapse of such a pulsar to a rotating black hole is a real possibility following dissipation of its rotational energy by magnetic dipole and/or gravitational radiation. In one of our models, corresponding to a soft equation of state, the rapidly rotating pulsar is actually seen to be spinning up right to the moment of its collapse!

Subject headings: pulsars — radiation mechanisms — stars: neutron — stars: rotation

I. INTRODUCTION

The observation of several millisecond radio pulsars has established the existence of rapidly rotating neutron stars. The recent report of 0.5 ms optical pulses from SN 1987A (Kristian *et al.* 1989), while now known to be spurious (Middleditch 1990), promoted the idea that neutron stars can in fact be born rapidly rotating (Sorrell 1989; Woosley and Chevalier 1989). Quite apart from these observations, Brecher and Chanmugam (1978, 1983) and Arons (1983) have discussed the birth of low magnetic field, rapidly rotating neutron stars in a general context. The direct observation of millisecond pulsars, and the anticipation of observing a submillisecond pulsar in SN 1987A, have stimulated considerable work recently on the physics of rapidly rotating neutron stars (Friedman, Iser, and Parker 1989; Shapiro, Teukolsky, and Wasserman 1989 and references therein).

The spin-down of a rapidly rotating pulsar is qualitatively different from that of a slowly rotating pulsar. For a slowly rotating star, the configuration is essentially spherical and loss of angular momentum J results in a decrease of the angular rotation rate Ω but no substantial change in the moment of inertia I . For a rapidly rotating star the configuration may be highly oblate, and the loss of angular momentum can result in a significant change in I . This change will affect the rate of spin-down for a given rate of angular momentum loss.

In this paper we demonstrate that the relationship between the rotation rate and the rotational distortion of a neutron star, and hence the rate of oblateness change and spin-down, is sensitive to the structure of the star. The structure in turn depends on the appropriate nuclear equation of state. Accordingly, spin-down measurements of a rapidly rotating pulsar may provide useful information about the global structure and/or microphysics of a neutron star.

Twenty years ago, Ostriker and Gunn (1969) quantitatively described the evolution of the Crab pulsar's period via dipole electromagnetic and quadrupole gravitational radiation energy loss. They adopted a simple vacuum oblique magnetic dipole model for the electromagnetic radiation (a nonvacuum aligned model would give a similar energy loss rate). They assumed that the dipole moment is constant in strength and orientation over the pulsar's entire life, and, most critically, that the pulsar was rotating much faster at birth than it is now. With this model they argued that neither electromagnetic nor gravitational radiation alone was sufficient to explain the Crab's current P , \dot{P} , and age, but that a suitable combination could be found to yield these values. Cowsik, Ghosh, and Melvin (1983) returned to the spin-down problem in the context of the 1.56 ms pulsar PSR 1937+214. They provided a

¹ Laboratory of Nuclear Studies, Department of Physics, Cornell University, Ithaca, NY 14853.

² Departments of Astronomy and Physics, Cornell University, Ithaca, NY 14853.

preliminary analysis of the effects of rotational distortion, but neglected gravitational radiation and only treated the evolution of incompressible fluid stars.

We reconsider the spin evolution of rapidly rotating neutron stars, modeling them as Maclaurin spheroids: uniform-density, rigidly rotating Newtonian fluid configurations in hydrostatic equilibrium. We endow our models with a magnetic moment μ and perturbative “mountain” of fractional height ϵ so that, as they rotate, they radiate energy and angular momentum via electromagnetic and gravitational waves. We also briefly consider gas accretion as a source of mass and angular momentum. The “hoop conjecture” (Thorne 1972) gives us a crude criterion by which we can determine which nonspherical models collapse to a black hole.

We confine our attention to *secularly stable* Maclaurin spheroids. These possess a limited range of angular momentum, with $T/|W|$ and eccentricity e satisfying

$$0 \leq T/|W| \leq 0.1375, \quad 0 \leq e \leq 0.812670, \quad (1)$$

where T is the rotational energy and W is the gravitational binding energy of the spheroid. Configurations with larger angular momentum J are subject to nonaxisymmetric bar-mode instabilities, driven by viscosity and/or gravitational radiation (cf. Chandrasekhar 1986, § 37). For typical parameters the period at the onset of the instability is quite short:

$$P \lesssim 0.66 \text{ ms} \left(\frac{M}{1.4 M_{\odot}} \right)^{-1/2} \left(\frac{a}{10 \text{ km}} \right)^{3/2}, \quad (2)$$

where a is the semimajor axis of one of our stellar models (an incompressible Maclaurin spheroid, described more fully in § II).

As our models evolve on slow electromagnetic dipole and gravitational radiation quadrupole time scales, they traverse a sequence of Maclaurin spheroids. All the properties of these spheroids are determined by their density ρ , mass M , and angular momentum J . The mass and the angular momentum are determined by accretion and/or radiation equations, leaving us the choice of density to fix the sequence. Each prescription for density determines a different sequence, and we consider two such sequences. First, we examine *incompressible* Maclaurin spheroids, for which the density does not change during spin-down. Subsequently, we progress to the more realistic sequence of *compressible* spheroids, where the (still uniform) density is related to the central pressure through a polytropic equation of state and changes during spin-down.

Even our compressible spheroids are highly idealized, especially compared with the fully general relativistic rapidly rotating neutron star models of Friedman, Ipser, and Parker (1986). Nevertheless, they provide a self-consistent, exact model of rotating equilibria. Their simplicity, in fact, is an advantage here: it allows us to explore the relationship between angular rotation and angular momentum more readily and in greater breadth than is now possible with fully relativistic, numerical models. We expect that, while some of the details resulting from a fully relativistic analysis would differ from those found here, the qualitative features we report below would remain.

In § II we examine the spin-down of neutron star models based on incompressible Maclaurin spheroids. We first develop a general set of equations for the spin evolution of these models, encompassing mass and angular momentum accretion as well as magnetic dipole and gravitational quadrupole radiation. We then specialize to radiation-driven spin-down, examining separately the electromagnetic and gravitational cases. We conclude our study of radiation spin-down of incompressible models with two applications: a model of the spin-down of a very rapidly rotating neutron star (born with period $P \sim 0.5$ ms), and an analysis of the Crab pulsar (PSR 0531 + 21) spin evolution. The latter is compared with the original Ostriker and Gunn (1969) calculation of the Crab pulsar’s spin evolution.

In § III we progress to the more realistic *compressible* models. After developing the equations describing the general spin evolution of these models (incorporating the effects of both accretion and radiation), we again restrict attention to radiation loss mechanisms and re-examine SN 1987A in more detail. We consider electromagnetic torques in isolation and combined electromagnetic and gravitational torques at the limits set by the observations of Kristian *et al.* (1989). We also consider the detectability of the resulting gravitational radiation. In § IV we return to the study of accretion spin-up, and consider gas accretion from an aligned Keplerian disk onto a weakly magnetized neutron star. Our conclusions are summarized in § V.

The parameters we adopt to describe the very rapidly rotating pulsar are taken to be illustrative. They were triggered by the spurious report of an 0.5 ms pulsar in SN 1987A and some of the theoretical discussion surrounding this object, as well as the original conclusions of Shapiro, Teukolsky, and Wasserman (1983) that the shortest period of a rotating neutron star consistent with currently viable equations of state is 0.5 ms (see also Friedman, Ipser, and Parker 1989; Shapiro, Teukolsky, and Wasserman 1989). For all cases we indicate appropriate scaling behaviors so that our calculations are generally applicable to other neutron stars with different periods.

II. INCOMPRESSIBLE MODELS

Here we employ constant-density sequences of Maclaurin spheroids with varying mass and angular momentum (owing to accretion, electromagnetic, and/or gravitational radiation) to describe the spin-down of rapidly rotating pulsars. After establishing the equations that govern the rate at which a neutron star progresses along such a sequence, we consider two applications: a pulsar born with an 0.5 ms period and the Crab pulsar.

a) Evolutionary Equations

The properties of oblate, homogeneous Maclaurin spheroids are summarized in Chandrasekhar (1986, § 2, 31–37) and Shapiro and Teukolsky (1983, hereafter ST, § 7.3). Central to their description is the relationship between the eccentricity e and the uniform

angular velocity of rotation Ω :

$$\Omega^2 = 2\pi\rho g(e), \quad (3)$$

$$g(e) \equiv \frac{(1-e^2)^{1/2}}{e^3} (3-2e^2) \sin^{-1} e - \frac{3(1-e^2)}{e^2} \quad (4)$$

(here and throughout this paper we adopt geometrized units where $G = c = 1$). The eccentricity establishes the relation between the semimajor (equatorial) axis a and the semiminor (polar) axis c according to $c = a(1-e^2)^{1/2}$. The angular velocity Ω of the spheroid is related to its angular momentum J through the moment of inertia I in the usual way,

$$J = I\Omega = \frac{2}{5}Ma^2\Omega, \quad (5)$$

and the (rest) mass is related to the density and the eccentricity according to

$$M = \frac{4\pi}{3} \rho a^3 (1-e^2)^{1/2}. \quad (6)$$

Equations (5) and (6) can be inverted to express a and I in terms of the mass, density, and eccentricity:

$$a = a_0(1-e^2)^{-1/6}, \quad a_0 \equiv \left(\frac{3M}{4\pi\rho}\right)^{1/3}, \quad (7a)$$

$$I = I_0(1-e^2)^{-1/3}, \quad I_0 = \frac{2}{5}Ma_0^2, \quad (7b)$$

where a_0 and I_0 are the radius and moment of inertia of a spherical, homogeneous star of the same mass M and density ρ as would result if the original spheroid radiated away all of its angular momentum at constant density.

With these relations, a Maclaurin spheroid is seen to be uniquely specified by its mass, density, and angular momentum, or equivalently by its mass, density, and eccentricity. Here we restrict attention to models of constant density. Consequently, the problem of describing the evolution of a stellar model reduces to determining the mass and eccentricity as functions of time. The variation of mass with time is described by the rate of accretion, \dot{M} , which in turn is determined by the properties of an accretion disk (for example). It remains to determine the evolution of eccentricity.

To describe the evolution of the eccentricity, take the logarithmic derivative of the equilibrium equations (3), (5), and (6):

$$2 \frac{d\Omega}{\Omega} = \frac{d\rho}{\rho} + \frac{g'(e)}{g(e)} de, \quad (8)$$

$$\frac{dJ}{J} = \frac{dM}{M} + 2 \frac{da}{a} + \frac{d\Omega}{\Omega}, \quad (9)$$

$$\frac{dM}{M} = \frac{d\rho}{\rho} + 3 \frac{da}{a} - \frac{e de}{1-e^2}. \quad (10)$$

For now, hold the density constant so that $d\rho/\rho$ vanishes (we shall relax this assumption in § III). Then equations (8), (9), and (10) may be combined to yield

$$\frac{\dot{J}}{J} - \frac{5}{3} \frac{\dot{M}}{M} = \frac{1}{2} \left(\frac{g'}{g} + \frac{4}{3} \frac{e}{1-e^2} \right) \dot{e}, \quad (11)$$

where a dot (as in \dot{J}) denotes a time derivative (dJ/dt) and a prime (as in g') denotes a derivative with respect to the eccentricity (dg/de). Noting that J (eq. [5]) is expressible in terms of M and e through equations (3) and (7b), we see that equation (11) describes the evolution of the eccentricity e , once the sources and sinks of mass and angular momentum (i.e., electromagnetic or gravitational radiation, or accretion) have been specified.

It is instructive to rewrite equation (11), replacing de/dt by $d\Omega/dt$:

$$\frac{\dot{J}}{J} - \frac{5}{3} \frac{\dot{M}}{M} = \frac{\dot{\Omega}}{\Omega} \left[1 + \frac{4}{3} \frac{g(e)e}{g'(e)(1-e^2)} \right]. \quad (12)$$

The second term in the brackets on the right-hand side is the correction to the standard spherical model for the evolution of the angular frequency of a pulsar. This term allows for nonspherical distortions (oblateness) owing to rotation, and for rapidly rotating pulsars it is of order unity and cannot be ignored.

Postponing the discussion of accretion until § IV, we consider two specific mechanisms of angular momentum loss: electromagnetic and gravitational radiation. For this purpose we endow our model pulsar with a test magnetic dipole moment μ and an ellipsoidal deformation of fractional magnitude ϵ . The projection of the magnetic moment perpendicular to the rotation axis is $\mu \sin \alpha$. The star continues to rotate about its semiminor axis, but cross sections normal to the rotation axis are slightly elliptical, with equatorial axes a and b such that

$$\epsilon \equiv \frac{a-b}{(a+b)/2} \quad (13)$$

(cf. ST, § 10.5 and 16.6).

The magnetic moment μ and fractional ellipsoidal deformation ϵ lead to energy and angular momentum loss via electromagnetic and gravitational radiation, respectively. Corresponding to this secular loss of energy from a rotating, equilibrium star is a loss of angular momentum according to

$$dE = \Omega dJ. \quad (14)$$

This is a general result proven by Ostriker and Gunn (1969) for Newtonian configurations of fixed mass, entropy, and chemical composition, and extended by Hartle (1970) to relativistic stars. For a Maclaurin spheroid, we can calculate the energy and angular momentum losses explicitly: the total energy of an incompressible spheroid is

$$E = W + T, \quad (15)$$

where W is the gravitational binding energy,

$$W \equiv -\frac{3}{5} \frac{M^2}{a} \frac{\sin^{-1} e}{e}, \quad (16)$$

and T is the rotational kinetic energy,

$$T = \frac{1}{2} I \Omega^2. \quad (17)$$

Equation (14) may be verified directly for incompressible Maclaurin spheroids by using equations (3) and (4) and (7a) and (7b) to express J , T , and W (eqs. [5], [16], and [17]) in terms of e , holding M and ρ fixed. It is then straightforward to show that dE/de and $\Omega dJ/de$ are equal.

According to equation (14), the energy loss rate immediately determines the time rate of change of angular momentum. For magnetic dipole radiation we have

$$\dot{E}_{\text{EM}} = -\frac{2}{3} |\ddot{\mu}|^2 = -\frac{2}{3} (\mu \sin \alpha)^2 \Omega^4, \quad (18)$$

and for gravitational quadrupole radiation

$$\dot{E}_{\text{GR}} = -\frac{1}{5} \left\langle \frac{d^3 I_{jk}}{dt^3} \frac{d^3 I_{jk}}{dt^3} \right\rangle = -\frac{32}{5} I^2 \epsilon^2 \Omega^6, \quad (19)$$

where I_{jk} is the reduced quadrupole moment (cf. ST, eq. [16.6.5] and discussion following), the angle brackets indicate an integration over all angles, and there is an implied summation over j and k . The corresponding rate of angular momentum loss due to electromagnetic and gravitational radiation is therefore

$$\dot{J} = \dot{J}_{\text{EM}} + \dot{J}_{\text{GR}}, \quad (20)$$

where

$$\dot{J}_{\text{EM}} = -\frac{2}{3} (\mu \sin \alpha)^2 \Omega^3 \equiv -\beta \Omega^3 \quad (21)$$

and

$$\dot{J}_{\text{GR}} = -\frac{32}{5} I^2 \epsilon^2 \Omega^5 = -\frac{32}{5} I_0^2 \epsilon^2 (1 - e^2)^{-2/3} \Omega^5 \equiv -\gamma_0 (1 - e^2)^{-2/3} \Omega^5. \quad (22)$$

In what follows, we assume that the projected magnetic moment $\mu \sin \alpha$ and fractional deformation ϵ remain constant. More generally, ϵ may be sensitive to the rotation rate of the neutron star, although the degree of sensitivity depends upon the rigidity of the crust and its “frozen-in” reference oblateness (cf. Pines and Shaham 1972; Alpar and Pines 1985). Then β and γ_0 are constant, and equation (11) may be written as

$$\frac{de}{dt'} = -\frac{\omega^4}{\pi} (1 - e^2)^{1/3} \left[1 + \frac{\lambda \omega^2}{(1 - e^2)^{2/3}} \right] \left[g'(e) + \frac{4}{3} \frac{g(e)e}{1 - e^2} \right]^{-1}, \quad (23)$$

where $t' = t/\tau$ is a dimensionless time, τ is the magnetic dipole damping time scale, ω is a dimensionless angular frequency, and $\lambda \omega^2$ relates the relative importance of gravitational and electromagnetic damping:

$$\tau \equiv \frac{I_0}{\beta \rho}, \quad (24a)$$

$$\omega \equiv \Omega/\rho^{1/2} = [2\pi g(e)]^{1/2}, \quad (24b)$$

$$\lambda \equiv \frac{\gamma_0 \rho_0}{\beta}. \quad (24c)$$

In the special case where there is no electromagnetic radiation ($\beta = 0$), we replace equation (23) with

$$\frac{de}{dt'} = -\frac{\omega^6}{\pi} (1 - e^2)^{-1/3} \left[g'(e) + \frac{4}{3} \frac{g(e)e}{1 - e^2} \right]^{-1}, \quad (25)$$

where again $t' = t/\tau$ but now

$$\tau \equiv \frac{I_0}{\gamma_0 \rho^2} \quad (26)$$

is the time scale for rotational damping by gravitational radiation.

b) Solutions

i) General Evolution

When there is no gravitational radiation ($\epsilon = 0$), equation (23) may be integrated without reference to any specific mass, density, or magnetic moment. The result is a “master curve” which describes how eccentricity varies with time for *any* model where the angular momentum loss is governed entirely by magnetic dipole radiation. The evolution of eccentricity describes the observed properties of a pulsar: the period, through equation (3), the period derivative $\dot{P} = -\dot{\Omega}/\Omega^2$, through

$$\dot{P} = -\frac{4\pi}{\tau \rho^{1/2}} \frac{g'(e)}{\omega^3} \frac{de}{dt'} \quad (27)$$

and equation (23); and the braking index,

$$n_B = \frac{\Omega \ddot{\Omega}}{\dot{\Omega}^2} = 2 - \frac{P \ddot{P}}{\dot{P}^2}. \quad (28)$$

An analytic expression for the braking index could also be found; however, we find it more convenient to determine the braking index numerically. Similarly, when there is no electromagnetic radiation ($\mu \sin \alpha = 0$), equation (25) may be integrated independently of M , ρ , and ϵ to obtain a second “master curve” that describes any model whose evolution is governed only by gravitational quadrupole radiation.

Figure 1 shows these two master curves. The solid and dashed lines are for stars with only electromagnetic and gravitational spin-down torques, respectively. The dotted and dot-dash curves show the equivalent master curves for the spin evolution of a

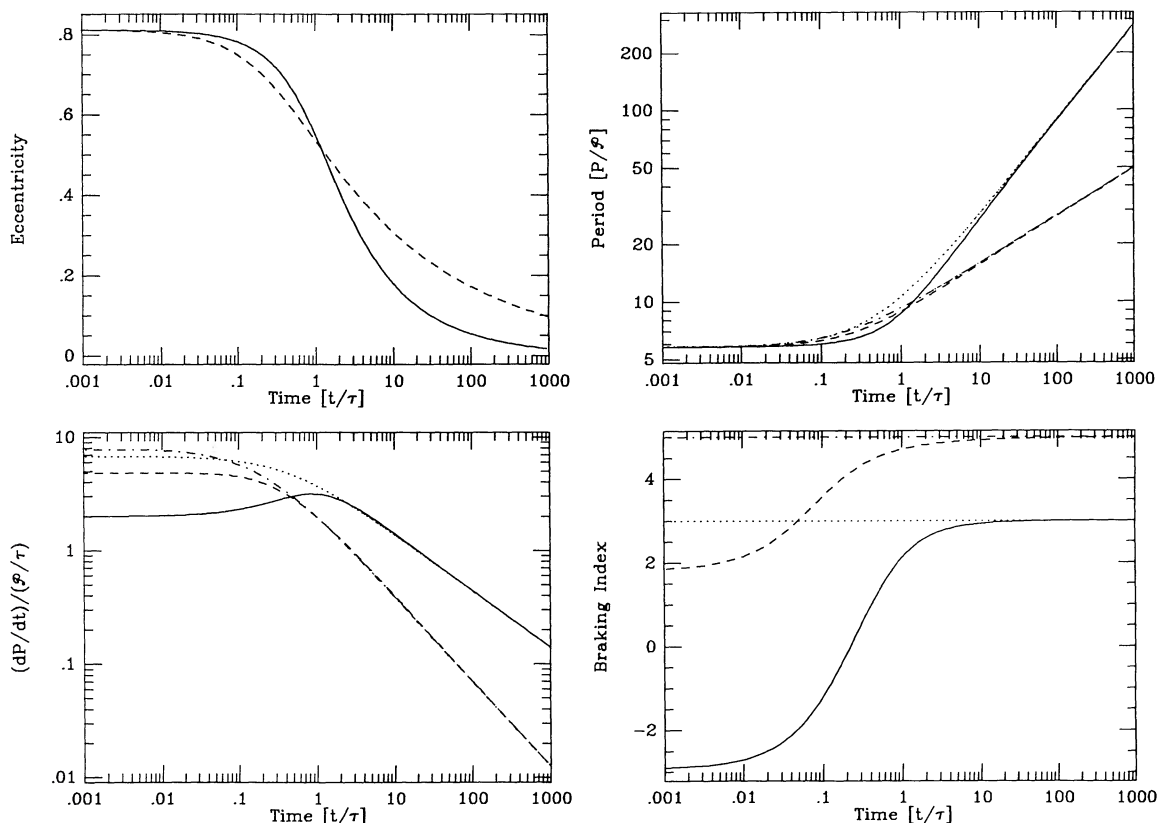


FIG. 1.—“Master curves” describing the spin evolution of the eccentricity e , period P , rate of period \dot{P} , and braking index n_B for a constant-density, constant-mass sequence of Maclaurian spheroids. The solid line describes the case of pure electromagnetic radiation spin-down with constant magnetic dipole moment, while the dashed line describes the case for pure quadrupole gravitational radiation with constant fractional ellipsoidal deformation. For comparison, the dotted (dot-dash) line shows the spin evolution of a *spherical* star for the case of pure electromagnetic (gravitational) radiation spin-down. Time is expressed in units of τ and period in units of \mathcal{P} , each of which depends on the moment of inertia, density, and strength of the radiation (see text). Note that only when the eccentricity becomes small does n_B settle into the usual value of 3 (5) for magnetic dipole (gravitational quadrupole) spin-down.

spherical star of the same mass and density with electromagnetic and gravitational spin-down torques, respectively. The time scale τ is given by equation (24a) for the electromagnetic and equation (26) for the gravitational master curve, and is related to the physical properties of specific models by

$$\tau = \begin{cases} 120 \text{ yr} \left(\frac{M}{1.4 M_{\odot}} \right)^{5/3} \left(\frac{3 \times 10^{14} \text{ g cm}^{-3}}{\rho} \right)^{5/3} \left(\frac{10^{30} \text{ G cm}^3}{\mu \sin \alpha} \right)^2 & \text{for } \epsilon = 0, \\ 0.24 \text{ yr} \left(\frac{M}{1.4 M_{\odot}} \right)^{-5/3} \left(\frac{3 \times 10^{14} \text{ g cm}^{-3}}{\rho} \right)^{4/3} \left(\frac{10^{-4}}{\epsilon} \right)^2 & \text{for } \mu \sin \alpha = 0. \end{cases} \quad (29)$$

We have normalized mass and density to mean values typical of neutron stars, and magnetic dipole moments to values inferred for typical strong field pulsars (corresponding to $B \simeq 10^{12}$ G). The “mountain height” parameter ϵ is normalized to a value consistent with the Ostriker and Gunn (1969) calculation of the spin evolution of the Crab pulsar (current thinking is that ϵ is considerably smaller than this value, as we shall see in § III). The origin of time is of course arbitrary; we have chosen it to correspond to the maximum eccentricity of a secularly stable Maclaurin spheroid ($e_{\text{sec}} = 0.812670$). For these constant- ρ models, this corresponds also to the maximum angular frequency during the evolution [$g'(e) > 0$ for $0 \leq e < e_{\text{sec}}$].

The upper left-hand panel of Figure 1 shows the variation of eccentricity with time for the pure electromagnetic and gravitational spin-down cases, while the upper right-hand panel shows how the period evolves for these cases. The units of the period are naturally related to the central density of a specific incompressible model:

$$\mathcal{P} = 1.4 \left(\frac{3 \times 10^{14} \text{ g cm}^{-3}}{\rho} \right)^{1/2} \text{ ms}. \quad (30)$$

The lower left-hand panel of Figure 1 shows how \dot{P} evolves with time. While \dot{P} is dimensionless, it does scale with the natural time and frequency of a specific model (eqs. [29], [30]), and we plot \dot{P} in units of \mathcal{P}/τ , where

$$\frac{\dot{P}}{\tau} = \begin{cases} 3.7 \times 10^{-13} \left(\frac{M}{1.4 M_{\odot}} \right)^{-5/3} \left(\frac{\rho}{3 \times 10^{14} \text{ g cm}^{-3}} \right)^{7/6} \left(\frac{\mu \sin \alpha}{10^{30} \text{ G cm}^3} \right)^2 & \text{for } \epsilon = 0, \\ 1.9 \times 10^{-10} \left(\frac{M}{1.4 M_{\odot}} \right)^{5/3} \left(\frac{\rho}{3 \times 10^{14} \text{ g cm}^{-3}} \right)^{5/6} \left(\frac{\epsilon}{10^{-4}} \right)^2 & \text{for } \mu \sin \alpha = 0. \end{cases} \quad (31)$$

The angular momentum J , eccentricity e , and moment of inertia I all decrease together. When the star is rapidly rotating and e is large, the change in dI is great and, for a given dJ , the corresponding dP is significantly smaller than it would be for a spherical star. For the electromagnetic case, we see that for large e , \dot{P} increases by 50% even as the star is spinning down. Correspondingly, for the same angular momentum the period of a rotationally distorted Maclaurin spheroid is greater than for a spherical star of the same M and ρ .

Viewed in another way, the rotational distortion is an angular momentum reservoir that is drained as the star spins down. In our incompressible models, the total angular momentum of the star is

$$J = I\Omega = I_0(1 - e^2)^{-1/3} [2\pi\rho g(e)]^{1/2}, \quad (32)$$

and the variation with eccentricity may be cast in the form

$$\frac{dJ}{de} = I \frac{d\Omega}{de} \left[1 + \frac{4}{3} \frac{eg(e)}{g'(e)(1 - e^2)} \right] \quad (33)$$

(cf. eq. [12]). If the star remained spherical as its angular momentum varied, then I would remain constant and the bracketed term would be unity. As it is, both I and the bracketed term increase with eccentricity; hence, for a given change in angular momentum, the change in angular velocity is smaller than for a spherical star, and this correction is larger the larger the eccentricity.

The effect of the changing rotational distortion is seen most vividly in the lower right-hand panel of Figure 1, which shows the braking index (cf. eq. [28]). For a spherical star, the braking index is a constant: exactly 3 for pure magnetic dipole spin-down torques and exactly 5 for gravitational quadrupole radiation torques (as is apparent from eqs. [21], [22], and [28]). The braking index, as shown in Figure 1, shows clearly that for large eccentricity \dot{P} is positive ($n_B < 2$) for both the electromagnetic and the gravitational cases.

ii) An 0.5 ms Pulsar

As an application of the electromagnetic master curves presented in the previous section, consider a rapidly rotating pulsar born with a period $P \sim 0.5$ ms (SN 1987A is a possible site for the birth of such a fast-spinning neutron star). In this subsection we examine its spin-down in terms of our incompressible Maclaurin spheroid model with strictly electromagnetic spin-down torques.

Suppose we assume that the pulsar was born with its maximum angular momentum, which in our model corresponds to an eccentricity $e_{\text{sec}} = 0.812670$, and that there has been no significant change in the period since birth. Then equation (3) immediately tells us that the density of the neutron star is $\rho = 2.0 \times 10^{15} \text{ g cm}^{-3}$. Suppose we also assume that the pulsar's mass is $1.7 M_{\odot}$, taking as our guide Friedman, Ipser, and Parker's (1989) argument that this must be the pulsar's approximate mass if any of the nuclear equations of state currently under consideration have any hope of being consistent with the observation. To determine the magnetic dipole moment, we need to fix the luminosity of the supernova. With the density, mass and initial eccentricity specified, the choice of magnetic moment $\mu \sin \alpha$ only affects the time scale over which the period changes (cf. eq. [24a]). We take a lower limit to

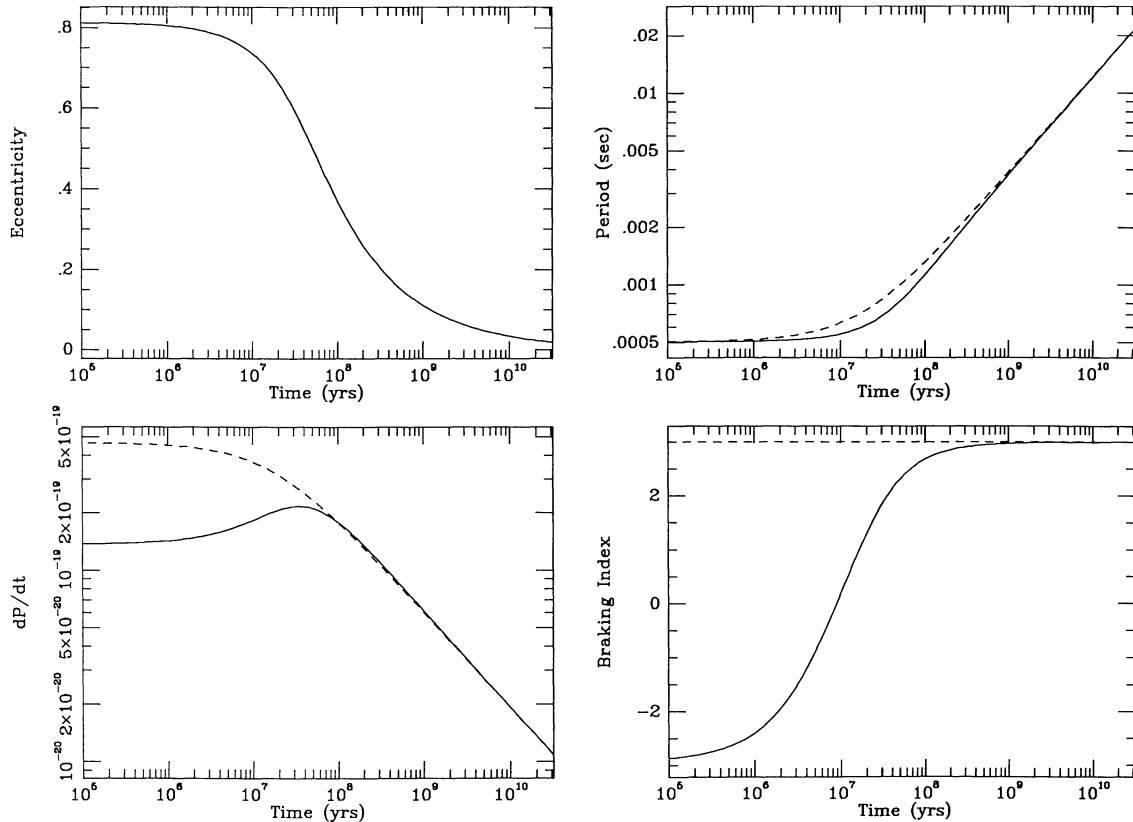


FIG. 2.—Spin evolution, by magnetic dipole radiation, of an incompressible Maclaurin spheroid model of a pulsar born with an 0.5 ms period (solid line). The mass, density, and magnetic dipole moment of the model were chosen to be consistent with observations of the pulsar and the supernova remnant. The oblateness of the spheroid at high rotation suppresses \dot{P} and dramatically affects P , \dot{P} , and the braking index n_b compared with the more conventional model in terms of a spherical star (dashed line).

that time scale by identifying the total luminosity of the SN 1987A remnant ($L \simeq 10^{38}$ ergs s^{-1} ; Middleditch *et al.* 1989) with the magnetic dipole radiation of the pulsar. This yields a projected magnetic moment $\mu \sin \alpha$ of 4.2×10^{26} G cm^3 . With these values for ρ , M , and $\mu \sin \alpha$, the time scale τ is

$$\tau = 4.0 \times 10^7 \text{ yr} \left(\frac{M}{1.7 M_{\odot}} \right)^{5/3} \left(\frac{2 \times 10^{15} \text{ g cm}^{-3}}{\rho} \right)^{5/3} \left(\frac{4.2 \times 10^{26} \text{ G cm}^3}{\mu \sin \alpha} \right)^2. \quad (34)$$

In Figure 2 the solid line is the electromagnetic master curve of the previous subsection, rescaled in physical units for this set of parameters, while the dashed line shows how the evolution would proceed for a *spherical* star of the same M , ρ , $\mu \sin \alpha$, and initial Ω . As discussed above, rotational distortion reduces \dot{P} at early times compared with the predictions of a spherical stellar model. If only magnetic dipole torques are acting on the pulsar, then our simple model suggests that present-day observations fall well within “early times.”

In choosing constant density, we have effectively chosen an incompressible equation of state for neutron star matter. In this limit, the semimajor axis of the star clearly increases with eccentricity, and the minimum is a_0 (cf. eq. [7a]). Applying the *hoop conjecture* (Thorne 1972) to this minimum radius, we find an approximate answer to the question of whether the star collapses to a black hole during the course of its spin-down. The hoop conjecture states that black holes with event horizons form when and only when a mass M gets compacted into a region whose circumference in every direction is $\mathcal{C} \leq 4\pi M$. Alternatively, if a star can pass through a “hoop” of radius $2M$ in any orientation, then it has collapsed to a black hole. Since the minimum equatorial radius that the oblate star would achieve is $a_0 = a(J=0)$, the radius reached when all the angular momentum has been radiated away, the hoop conjecture suggests that it collapses to form a black hole during spin-down only if $a_0 < 2M$. For the incompressible model considered here $a_0/2M = 1.5$, and a black hole is not formed. Nevertheless, it settles into a very compact final configuration. In § III we describe models with compressible equations of state, finding that for these more realistic models of an 0.5 ms pulsar, catastrophic collapse is not only possible but likely.

iii) The Crab Pulsar

As a second application of our simple incompressible model, we reanalyze the Ostriker and Gunn (1969, hereafter OG) calculation of the spin evolution of the Crab pulsar. Given its age and present-day values of P and \dot{P} , OG found the projected magnetic moment $\mu \sin \alpha$ and fractional mountain height ϵ as a function of the star’s initial angular velocity and moment of inertia, which they took to be a constant. The calculation we carry out below differs from theirs in two respects: (i) our model accounts for the large

variation of the moment of inertia at rapid rotation rates, and (ii) we assume that at birth the Crab had the maximum permissible angular momentum (corresponding to an eccentricity e_{sec}).

In the OG calculation, two equations determine the magnetic moment and the mountain height commensurate with a given I_0 . Introduce

$$\tilde{\lambda} \equiv \frac{\gamma_0 \Omega_0^4}{\beta} \quad \text{and} \quad \tilde{\mu} \equiv \left(\frac{\Omega_0}{\Omega_i} \right)^2, \quad (35)$$

with β and γ_0 given by equations (21) and (22); let T_{Crab} be the age of the Crab (e.g., 918 yr in 1972); and let Ω_0 and $\dot{\Omega}_0$ be the angular frequency and its rate at the current epoch ($\Omega_0 = 190$ Hz, $\dot{\Omega}_0 = -2.42 \times 10^{-9}$ s $^{-2}$ in 1972). Then β and γ_0 are found by satisfying the two equations

$$(1 + \tilde{\lambda}) \left(1 - \tilde{\mu} + \tilde{\lambda} \log \frac{\tilde{\lambda} + \tilde{\mu}}{\tilde{\lambda} + 1} \right) = -2T_{\text{Crab}} \frac{\dot{\Omega}_0}{\Omega_0} \quad (36)$$

and

$$\frac{\beta \Omega_0^2}{I_0} (1 + \tilde{\lambda}) = -\frac{\dot{\Omega}_0}{\Omega_0} \quad (37)$$

(cf. ST, § 10.5). Equation (36) comes from integrating equation (12) in time, using equations (20)–(22) with $dM = 0$ and $e = 0$ (spherical limit). Equation (37) arises from equation (9) with $dM = da = 0$ and equations (20)–(22). Once a value of $\tilde{\mu}$ is chosen, the first equation is a transcendental equation for $\tilde{\lambda}$ and the second determines β from $\tilde{\lambda}$. Once β is determined, ϵ follows from $\tilde{\lambda}$ and the definition of γ_0 (eq. [22]).

To draw the correspondence between the OG calculation and our own, we assume that the constant moment of inertia used in their calculation corresponds to our I_0 (cf. eqs. [7b]); thus, we identify the OG model with the slow rotation (spherical star) limit of our own. In our nonspherical model, in contrast to the OG calculation, we cannot obtain an analytic, or even a transcendental, equation whose roots provide the β and ϵ that go with a given choice of I_0 and Ω_i . Instead, having chosen ρ and M (equivalent to choosing I_0 and a_0 ; cf. eqs. [7b]), and Ω_i , we must search numerically for β and ϵ in the following fashion:

1. Together with ρ , Ω_0 determines e_0 , the eccentricity today, through equation (3).
2. Pick a (β, ϵ) pair such that Ω takes on the desired value Ω_0 (cf. eq. [12]). This also determines λ (cf. eq. [24c]) in equation (23).
3. The initial angular rotation rate Ω_i determines the initial eccentricity e_i and allows us to integrate equation (23) until $e = e_0$.

The elapsed time is the age of the pulsar. If it does not agree with T_{Crab} , then pick a new β, ϵ pair and try again.

This search of a two-dimensional parameter space is simplified by noting that only at early times when the rotation is rapid will the evolution of the Crab differ significantly between the OG model and our own; consequently, since the Crab is now slowly rotating, the OG model provides good estimates for the magnetic moment and mountain height for our more general, nonspherical model.

Figure 3 shows the evolution of a star with $I_0 = 1.4 \times 10^{45}$ g cm 2 and $a_0 = 12$ km (corresponding to $M = 1.22 M_\odot$ and $\rho = 3.36 \times 10^{14}$ g cm $^{-3}$) for both the OG model (*dashed line*) and our own (*solid line*). The initial angular velocity was chosen so that the initial eccentricity was at its maximum, $e = e_{\text{sec}}$. The magnetic moment and mountain height for the two models did not differ significantly: for our model $\mu \sin \alpha = 3.9675 \times 10^{33}$ G cm 3 and $\epsilon = 2.920 \times 10^{-4}$, while for the OG model $\mu \sin \alpha = 3.9678 \times 10^{33}$ G cm 3 and $\epsilon = 2.914 \times 10^{-4}$. As expected, at very early times (compared to the Crab's present age) there are significant differences between these models (cf. the braking index and \dot{P} in Fig. 3); however, since the Crab has been rotating slowly compared with its maximum angular velocity for many years now, there are no longer any significant observational differences between the two models.

III. COMPRESSIBLE MODELS

In the previous section we focused on constant-density evolutionary sequences of Maclaurin spheroids. Here we consider more general models where the density varies during the star's evolution. We assume that the central pressure is related to the density according to a realistic polytropic equation of state. As an application we examine the spin-down of PSR 1987A, paying special attention to the gravitational radiation from the pulsar as well as the question of its final state.

The rate at which a star loses angular momentum as a result of magnetic dipole radiation depends upon its projected magnetic dipole moment $\mu \sin \alpha$. If the magnetic flux is frozen into the surface of the pulsar, then, as the pulsar's oblateness changes, so does its magnetic moment. In the last subsection below, we incorporate flux freezing in a model calculation, thereby replacing our earlier assumption of constant dipole moment.

a) Evolutionary Equations

Maclaurin spheroids are constrained to be homogeneous; however, we can choose the uniform density any way we wish. In particular, we can make it a function of the central equilibrium pressure P_c according to a prescribed equation of state. The central pressure of a Maclaurin spheroids is determined by integrating the equation of hydrostatic equilibrium, and is (cf. ST, § 7.3)

$$P_c = \pi \rho^2 a^2 (1 - e^2) A_3(e), \quad (38)$$

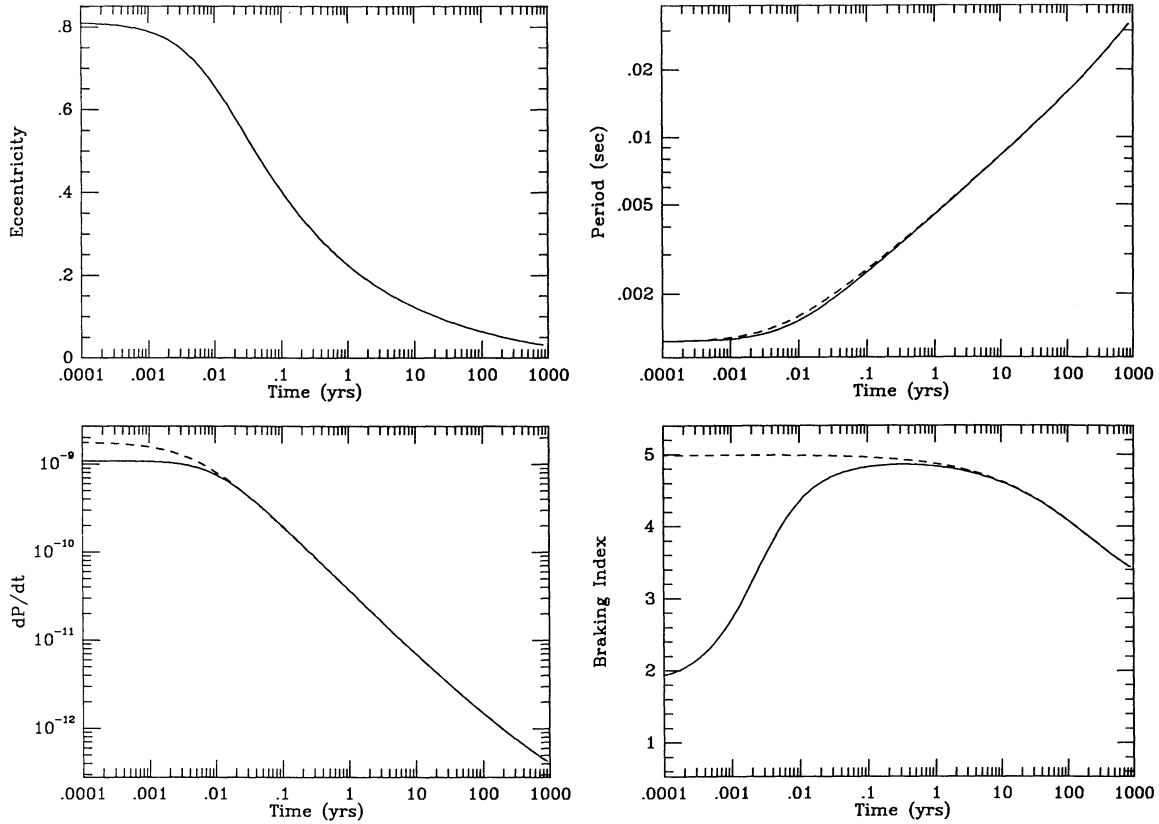


FIG. 3.—The Ostriker-Gunn (1969) calculation of the spin evolution of the Crab pulsar suggests that at early times it was rotating rapidly, and so highly oblate. The solid line shows the spin evolution of an incompressible Maclaurin spheroid model of the Crab pulsar, while the dashed line shows the results of the Ostriker-Gunn (1969) calculation for a spherical star.

where

$$A_3(e) \equiv \frac{2}{e^2} \left[1 - (1 - e^2)^{1/2} \frac{\sin^{-1} e}{e} \right]. \quad (39)$$

Here we shall consider polytropic equations of state:

$$P_c = \mathcal{K} \rho_{\text{ref}} \left(\frac{\rho}{\rho_{\text{ref}}} \right)^\Gamma. \quad (40)$$

The sound speed is

$$c_s^2 \equiv \frac{dP}{d\rho} = \frac{\Gamma P_c}{\rho}, \quad (41)$$

and ρ_{ref} is a reference density at which $\Gamma \mathcal{K}$ is the squared sound speed. Density is now a function of eccentricity given by combining equation (40) with equation (38):

$$\left(\frac{\rho}{\rho_{\text{ref}}} \right)^{\Gamma-2} = \pi(1 - e^2) A_3 \rho_{\text{ref}} a^2 \mathcal{K}^{-1}. \quad (42)$$

It is convenient to introduce ρ_0 , the density at $e = 0$ of a spherical model with same mass M ,

$$\left(\frac{\rho_0}{\rho_{\text{ref}}} \right)^{\Gamma-4/3} \equiv \frac{2}{3} \frac{\pi}{\mathcal{K}} \left(\frac{3}{4\pi} \right)^{2/3} (\rho_{\text{ref}} M^2)^{1/3}. \quad (43)$$

Then

$$\left(\frac{\rho}{\rho_0} \right)^{\Gamma-4/3} = \frac{3}{2} (1 - e^2)^{2/3} A_3(e), \quad (44)$$

and we can generalize our earlier definitions of I_0 and a_0 (eqs. [7a] and [7b]) to these more sophisticated compressible models:

$$a = a_0 \left(\frac{\rho_0}{\rho} \right)^{1/3} (1 - e^2)^{-1/6}, \quad a_0 \equiv \left(\frac{3M}{4\pi\rho_0} \right)^{1/3}, \quad (45a)$$

$$I = I_0 \left(\frac{\rho_0}{\rho} \right)^{2/3} (1 - e^2)^{-1/3}, \quad I_0 \equiv \frac{2}{5} M a_0^2. \quad (45b)$$

So defined, ρ_0 , a_0 , and I_0 are the density, radius, and moment of inertia of a spherical, uniform-density star of mass M whose central pressure satisfies the equation of the state (40). In the limit $\Gamma \rightarrow \infty$ (corresponding to polytropic index $n = 0$, where $\Gamma = 1 + 1/n$) and $\rho \rightarrow \rho_0$, these reduce to the definitions we used for the incompressible models (cf. eqs. [7a] and [7b]).

Since ρ now varies with the time-varying eccentricity of a model, equation (11) no longer describes its evolution along a sequence. To generalize equation (11), combine equations (8), (9), and (10) with the logarithmic derivative of equation (42),

$$(\Gamma - 2) \frac{d\rho}{\rho} = 2 \frac{da}{a} + \left(\frac{A'_3}{A_3} - \frac{2e}{1 - e^2} \right) de, \quad (46)$$

to obtain

$$\frac{\dot{J}}{J} - \left(\frac{5}{3} - \frac{1/3}{3\Gamma - 4} \right) \frac{\dot{M}}{M} = \frac{1}{2} \left\{ \frac{g'}{g} + \frac{1}{3\Gamma - 4} \left[\frac{4(\Gamma - 1)e}{1 - e^2} - \frac{A'_3}{A_3} \right] \right\} \frac{de}{dt}. \quad (47)$$

It is also useful to find the corresponding equation for $\dot{\Omega}$, which we give here for the case $\dot{M} = 0$:

$$\frac{\dot{J}}{J} = \frac{\dot{\Omega}}{\Omega} \left\{ 1 + \frac{4}{3\Gamma - 4} \left(\frac{\Gamma e}{1 - e^2} - \frac{A'_3}{A_3} \right) \left[\frac{g'}{g} + \frac{1}{3\Gamma - 4} \left(\frac{3A'_3}{A_3} - \frac{4e}{1 - e^2} \right) \right]^{-1} \right\} \quad (48)$$

Like the incompressible models, at each moment of the time these compressible models are in hydrostatic equilibrium. Angular momentum changes on radiation loss time scales, which are long compared with the hydrodynamic time scales that control the shape of the configuration; hence, virial theorems control the distribution of energy between internal, gravitational binding, and bulk kinetic forms. Each star moves along its sequence quasi-statically, and so the relationship between energy loss and angular momentum loss is again given by equation (14).

$$E = W + T + T_{\text{int}}, \quad (49)$$

where W and T are defined as before (cf. eqs. [16] and [17]) and the internal energy is given by

$$T_{\text{int}} = \frac{2}{5} \frac{1}{\Gamma - 1} \frac{P_c}{\rho} M. \quad (50)$$

Incidentally, while it is trivial to verify equation (14) for the incompressible models of § II, it is a nontrivial algebraic exercise to show that it also holds true for the more complicated compressible models where the internal energy plays a role and the density can vary. While straightforward, this computation was of sufficient complexity that to carry it through we resorted to the use of the algebraic manipulator Maple running on the Cornell National Supercomputing Facilities IBM 3090/600E.

We postpone further discussion of accretion until § IV and consider here only electromagnetic and gravitational radiation spin-down torques. The rates of energy and angular momentum loss are still given by equations (14), (21), and (22), however, we must generalize the definition of γ_0 so that it remains constant for our compressible models:

$$j_{\text{GR}} = -\frac{32}{5} I^2 \epsilon^2 \Omega^5 \equiv -\gamma_0 \left(\frac{\rho_0}{\rho} \right)^{4/3} (1 - e^2)^{-2/3} \Omega^5. \quad (51)$$

Assuming constant $\mu \sin \alpha$ and ϵ , γ_0 and β (cf. eq. [21]) are constant and the evolution of eccentricity is now described by

$$\frac{de}{dt'} = -\frac{\omega^4}{\pi} \left(\frac{\rho_0}{\rho} \right)^{1/3} (1 - e^2)^{1/3} \left[1 + \left(\frac{\rho_0}{\rho} \right)^{4/3} \frac{\lambda \omega^2}{(1 - e^2)^{2/3}} \right] \left\{ g'(e) + \frac{g(e)}{3\Gamma - 4} \left[\frac{4(\Gamma - 1)e}{1 - e^2} - \frac{A'_3}{A_3} \right] \right\}^{-1}, \quad (52)$$

where $t' = t/\tau$ is a dimensionless time, and

$$\tau \equiv \frac{I_0}{\rho_0 \beta}, \quad (53a)$$

$$\lambda \equiv \frac{\gamma_0 \rho_0}{\beta}, \quad (53b)$$

$$\omega \equiv \Omega \rho_0^{-1/2}. \quad (53c)$$

Again, equation (52) reduces to equation (23) when $\Gamma \rightarrow \infty$. In the special case where there is no electromagnetic radiation [$\beta = 2(\mu \sin \alpha)^2/3 = 0$] we write

$$\frac{de}{dt'} = -\frac{\omega^6}{\pi} \left(\frac{\rho_0}{\rho}\right)^{5/3} (1-e^2)^{-1/3} \left\{ g'(e) + \frac{g(e)}{3\Gamma-4} \left[\frac{4(\Gamma-1)e}{1-e^2} - \frac{A'_3}{A_3} \right] \right\}^{-1}, \quad (54)$$

where

$$\tau \equiv \frac{I_0}{\rho_0^2 \gamma_0}. \quad (55)$$

As with the incompressible models, the variation of eccentricity with time determines all other properties of the star. In the case of pure electromagnetic or gravitational radiation spin-down torques, integrating either of equations (52), and (54) only requires specification of Γ . If there are both electromagnetic and gravitational spin-down torques, then λ must also be specified. No other information about the specific stellar model or equation of state need be given. Thus, in general there is a two-parameter family of sequences (λ and Γ) that describe the evolution by electromagnetic and gravitational radiation torques of all models with equation of state (40). Once these curves are determined, the choice of a mass, a sound speed at some reference density ($\Gamma \mathcal{K}$ at ρ_{ref}), and a magnetic dipole moment $\mu \sin \alpha$ or mountain height ϵ completely determine the rest of the model.

Consider the secular stability properties of compressible Maclaurin spheroids. Recall that along the usual sequences of incompressible Maclaurin spheroids, the eccentricity $e_{sec} = 0.812670$ is a point of bifurcation where the sequence of Jacobi ellipsoids branches off (cf. Chandrasekhar 1986, §§ 3, 39). The bifurcation point itself depends only on equilibrium relations and geometrical constraints and is independent of the nature of the sequence (e.g., constant density vs. eq. [40]). We must still check that the total energy of compressible Jacobi ellipsoids (including the internal energy) is always greater than or equal to that of the corresponding $e = e_{sec}$ compressible Maclaurin spheroid; otherwise, Maclaurin spheroids with $e < e_{sec}$ might be unstable to triaxial deformation. We have verified that this inequality holds true and that the total energy of compressible Jacobi ellipsoids increases with angular momentum. Consequently, there can be no instability that leads compressible Maclaurin spheroids with $e < e_{sec}$ to evolve to Jacobi ellipsoids. For reference, the three contributions (gravitational, rotational, and internal) to the total energy for a compressible triaxial ellipsoid are

$$W = -\frac{3}{10} \frac{M^2}{a_1} \frac{I_{Ch}}{a_2 a_3}, \quad (56)$$

$$T_{int} = \frac{1}{\Gamma-1} \frac{M^2}{a_1} \left(\frac{3}{4} \frac{a_3}{a_2} A_3 + \frac{3}{20} \frac{a_1^2 + a_2^2}{a_2 a_3} B_{12} - \frac{3}{20} \frac{I_{Ch}}{a_2 a_3} \right), \quad (57)$$

$$T = \frac{3}{20} \frac{M^2}{a_1} \frac{a_1^2 + a_2^2}{a_2 a_3} B_{12}, \quad (58)$$

where $a_1 > a_2 > a_3$ are the three principal axes of the ellipsoid,

$$I_{Ch} \equiv \sum_{i=1}^3 A_i a_i^2, \quad (59)$$

and A_1, A_2, A_3 , and B_{12} are index symbols defined in Chandrasekhar (1986; cf. §§ 17 and 21). For the Maclaurin sequence these may be written in the form

$$W = \frac{3}{5} \frac{M^2}{a_0} \left(\frac{\rho}{\rho_0}\right)^{1/3} \frac{\sin^{-1} e}{e} (1-e^2)^{1/6}, \quad (60)$$

$$T_{int} = \frac{3/10}{\Gamma-1} \frac{M^2}{a_0} A_3(e) \left(\frac{\rho}{\rho_0}\right)^{1/3} (1-e^2)^{2/3}, \quad (61)$$

$$T = \frac{3}{10} \frac{M^2}{a_0} \left(\frac{\rho}{\rho_0}\right)^{1/3} (1-e^2)^{-1/3} g(e). \quad (62)$$

The energy of the incompressible models in the last section is given by these equations in the limit $\Gamma \rightarrow \infty, \rho \rightarrow \rho_0$. Again, note that in this limit the internal energy vanishes.

b) Collapse to a Black Hole

As before, we use the hoop conjecture (Thorne 1972) to determine when one of our evolving models has collapsed to a black hole. For the incompressible models it is clear by inspection that the semimajor axis a is a monotonic increasing function of the eccentricity (cf. eqs. [7a]); hence we can determine whether an oblate model collapses to a black hole by checking its semimajor radius at zero eccentricity, after all the angular momentum has been radiated away. For the more general compressible models it is no longer obvious that a is a monotonically increasing function of eccentricity. Nevertheless, we can still show analytically that for all $\Gamma > 4/3$, $a/2M$ is monotonically increasing with e ; consequently, a_0 is still a diagnostic of black hole formation during the

spin-down of a neutron star. In particular, we can find a condition for eventual black hole collapse based on the softness of the adiabatic index:

$$\Gamma - \frac{4}{3} < \Gamma_{\text{crit}} - \frac{4}{3} = \frac{\log [2(1 - e^2)^{2/3}/3A_3(e)]}{\log [(32\pi/3)M^2\rho_0(1 - e^2)^{-1/2}]} \Leftrightarrow \text{Black hole} \quad (63)$$

for some value $1 > e > 0$.

c) An 0.5 ms Pulsar Revisited

As an application of the compressible Maclaurin models, consider again the spin-down by magnetic dipole radiation of a pulsar born with an 0.5 ms period. As before, fix $M = 1.7 M_{\odot}$, and insist that the initial observed rotation rate of 2000 Hz be matched with the maximum eccentricity of a stable Maclaurin spheroid $e_{\text{sec}} = 0.812670$. This determines the initial density (cf. eq. [3]) and, once Γ is specified, the equation of state (cf. eqs. [43] and [44]):

$$\mathcal{K} = \frac{3}{4} \left(\frac{4\pi}{3} \right)^{1/3} (1 - e_{\text{sec}}^2)^{2/3} A_3(e_{\text{sec}}) (M^2 \rho_{\text{ref}})^{1/3} \left[2\pi g(e) \frac{\rho_{\text{ref}}}{\Omega^2} \right]^{\Gamma - 4/3} \quad (64)$$

$$= 0.12 \left(\frac{M}{1.7 M_{\odot}} \right)^{2/3} \left(\frac{\rho_{\text{ref}}}{2.0 \times 10^{15} \text{ g cm}^{-3}} \right)^{\Gamma - 1} \left(\frac{P}{0.5 \text{ ms}} \right)^{2(\Gamma - 4/3)} \quad (65)$$

The only remaining free parameter, $\mu \sin \alpha$, determines the time scale over which the evolution takes place. As before (cf. § I Ib[ii]), we choose the projected magnetic moment by assuming that the pulsar is responsible for the remnant's total observed luminosity: $\mu \sin \alpha = 4.2 \times 10^{26} \text{ G cm}^3$.

With everything but Γ fixed, the results of the previous subsection tell us that a black hole forms during spin-down if $a_0/2M < 1$ or

$$\Gamma - 4/3 < \Gamma_{\text{crit}} - 4/3 = 0.293 \quad (66)$$

Thus, for these parameters we find that collapse to a black hole is inevitable for almost all equations of state softer than a Fermi gas of free neutrons.

Figure 4 shows the evolutionary paths of compressible Maclaurin models for three choices of Γ . The solid line, corresponding to $\Gamma = 5/3$, has the stiffness of a nonrelativistic Fermi gas and does not end its life as a black hole. The dotted line corresponds to a model with a slightly softer equation of state ($\Gamma - 4/3 = 0.29$). This model ends its life in a black hole (marked by a filled circle). The dashed line corresponds to a model with a very soft equation of state ($\Gamma - 4/3 = 0.1$) and collapses to a black hole at an even higher eccentricity.

The models shown in Figure 4 are quite startling, because each one begins its life with a *negative* \dot{P} : as these stars lose angular momentum, their moments of inertia initially decrease so rapidly that they spin *up* in the same way that a skater spins faster as his or her arms are drawn inward. The model with the softest equation of state (the dashed line, corresponding to $\Gamma - 4/3 = 0.1$) spins up at an ever-increasing rate up until the moment it collapses to a black hole with nearly half its original period! The resulting Kerr black hole has an angular momentum parameter $a/M = 0.24$.

We have also examined the spin evolution of these models by simultaneous gravitational and electromagnetic radiation. For our calculations we chose the deformation $\epsilon = 5 \times 10^{-7}$ about which we scale all of our results. For comparison, Pines and Shaham (1972) find that $\epsilon \lesssim 10^{-6}$ is a reasonable triaxial deformation for a neutron star. Figure 5 shows the results of these calculations. Note that, owing to the rapid rotation, the observed upper bound on $|\dot{P}|$ severely constrains ϵ . It must be appreciably lower than the value required by the OG model of the Crab pulsar, for example (cf. § I Ib[iii]).

The amplitude of the gravitational radiation from a triaxial, rapidly rotating neutron star is also affected by its evolving shape. Since the radiation is periodic and monochromatic, both bar and interferometric detectors can achieve high sensitivity by prolonged observation (cf. Thorne 1987). In order to evaluate the radiation from our models, we introduce a stationary spherical-polar coordinate system centered on the rotating neutron star, with the polar and symmetry axes coincident. An observer viewing the neutron star from the θ , ϕ direction can resolve the gravitational radiation field into two polarization components. These are commonly referred to as the "plus" and "cross" polarization states and are expressed as

$$h_{ij}^{TT} \mathbf{e}_i \otimes \mathbf{e}_j \equiv h_+ \mathbf{e}_+ + h_{\times} \mathbf{e}_{\times} \quad (67)$$

where the basis tensors \mathbf{e}_+ and \mathbf{e}_{\times} are given in terms of the orthonormal basis vectors $\mathbf{e}_{\hat{r}}$, $\mathbf{e}_{\hat{\theta}}$, and $\mathbf{e}_{\hat{\phi}}$ according to

$$\mathbf{e}_+ \equiv \mathbf{e}_{\hat{\theta}} \otimes \mathbf{e}_{\hat{\theta}} - \mathbf{e}_{\hat{\phi}} \otimes \mathbf{e}_{\hat{\phi}} \quad (68a)$$

$$\mathbf{e}_{\times} \equiv \mathbf{e}_{\hat{\theta}} \otimes \mathbf{e}_{\hat{\phi}} + \mathbf{e}_{\hat{\phi}} \otimes \mathbf{e}_{\hat{\theta}} \quad (68b)$$

In the quadrupole approximation, the gravitational radiation field is given in terms of the trace reduced quadrupole moment I_{ij} ,

$$h_{ij}^{TT} = \frac{2}{r} \ddot{I}_{ij}^{TT} \quad (69)$$

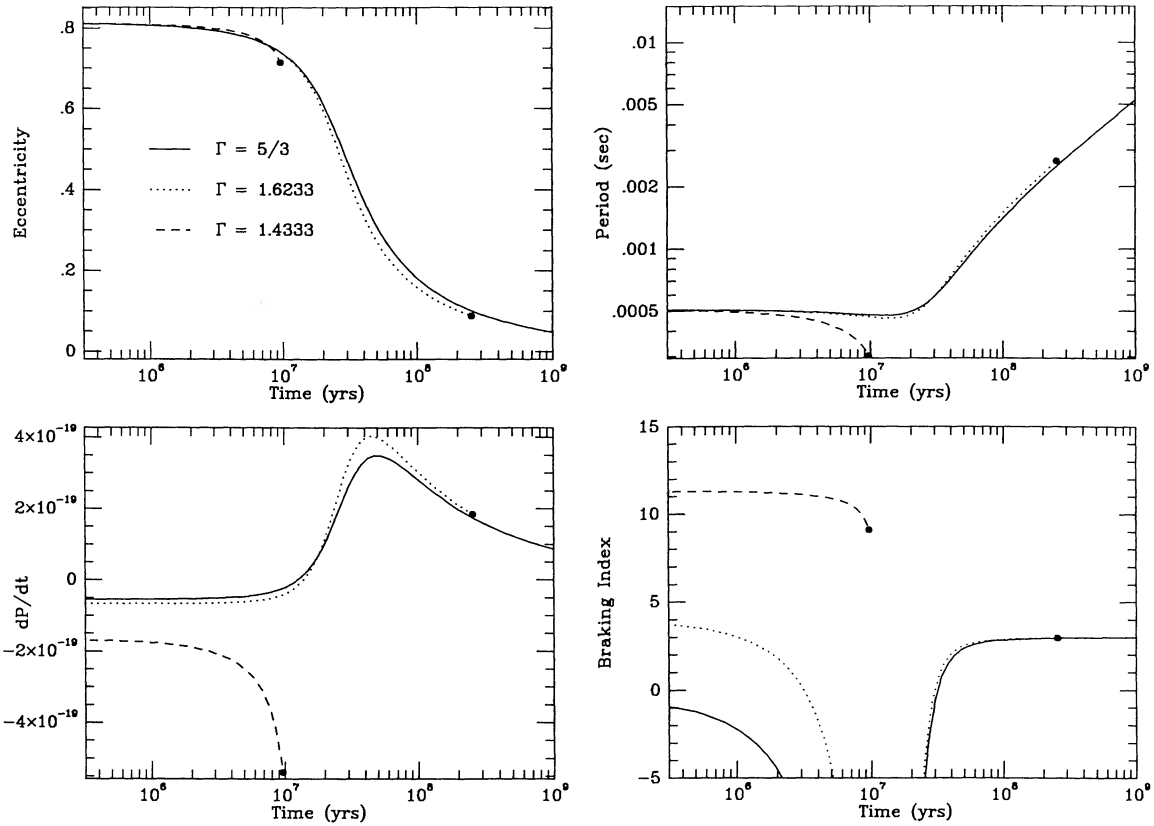


FIG. 4.—Spin evolution, via magnetic dipole radiation, of a compressible Maclaurin spheroid model of an initially 0.5 ms pulsar. Cases corresponding to three different polytropic equations of state, parameterized by the polytropic index, are shown here. Note how all the models show a negative \dot{P} at early times, corresponding to spin-up, even as they are losing angular momentum. The sequences corresponding to the two softest equations of state form black holes at finite times, indicated by filled circles. The model corresponding to the softest equation of state is rotating at nearly half its period at birth and still has a negative \dot{P} at the time of its collapse to a black hole.

(Misner, Thorne, and Wheeler 1973), or

$$h_+ = \frac{1}{r} (\ddot{I}_{\theta\theta} - \ddot{I}_{\phi\phi}), \quad (70a)$$

$$h_x = \frac{2}{r} \ddot{I}_{\theta\phi}. \quad (70b)$$

The components $\ddot{I}_{\theta\theta}$, $\ddot{I}_{\theta\phi}$ and $\ddot{I}_{\phi\phi}$ are expressible in terms of the Cartesian components of \ddot{I}_{ij} as

$$\ddot{I}_{\theta\theta} = (\ddot{I}_{xx} \cos^2 \phi + \ddot{I}_{yy} \sin^2 \phi + \ddot{I}_{xy} \sin 2\phi) \cos^2 \theta + \ddot{I}_{zz} \sin^2 \theta - (\ddot{I}_{xz} \cos \phi + \ddot{I}_{yz} \sin \phi) \sin 2\theta, \quad (71a)$$

$$\ddot{I}_{\phi\phi} = \ddot{I}_{xx} \sin^2 \phi + \ddot{I}_{yy} \cos^2 \phi - \ddot{I}_{xy} \sin 2\phi, \quad (71b)$$

$$\ddot{I}_{\theta\phi} = -\frac{1}{2}(\ddot{I}_{xx} - \ddot{I}_{yy}) \cos \theta \sin 2\phi + \ddot{I}_{xy} \cos \theta \cos 2\phi + (\ddot{I}_{xz} \sin \phi - \ddot{I}_{yz} \cos \phi) \sin \theta \quad (71c)$$

(Kochanek *et al.* 1990).

Equations (70a)–(70b) and (71a)–(71c) are completely general for any Newtonian source of gravitational radiation. We now specialize to triaxial rotating models. Shapiro and Teukolsky (1983, § 16.6) give the Cartesian components of the moment-of-inertia tensor I_{ij} , and, substituting these into equations (71a)–(71c) and then (70a)–(70b), we find

$$h_+ \equiv \frac{1}{r} \frac{2}{5} M(a+b)^2 \epsilon \Omega^2 \frac{\cos^2 \theta + 1}{2} \cos [2(\phi - \Omega t)] \quad (72a)$$

$$\simeq \frac{4\epsilon}{r} \Omega^2 I \frac{\cos^2 \theta + 1}{2} \cos [2(\phi - \Omega t)], \quad (72b)$$

$$h_x \equiv -\frac{1}{r} \frac{2}{5} M(a+b)^2 \epsilon \Omega^2 \cos \theta \sin [2(\phi - \Omega t)] \quad (72c)$$

$$\simeq -\frac{4\epsilon}{r} \Omega^2 I \cos \theta \sin [2(\phi - \Omega t)], \quad (72d)$$

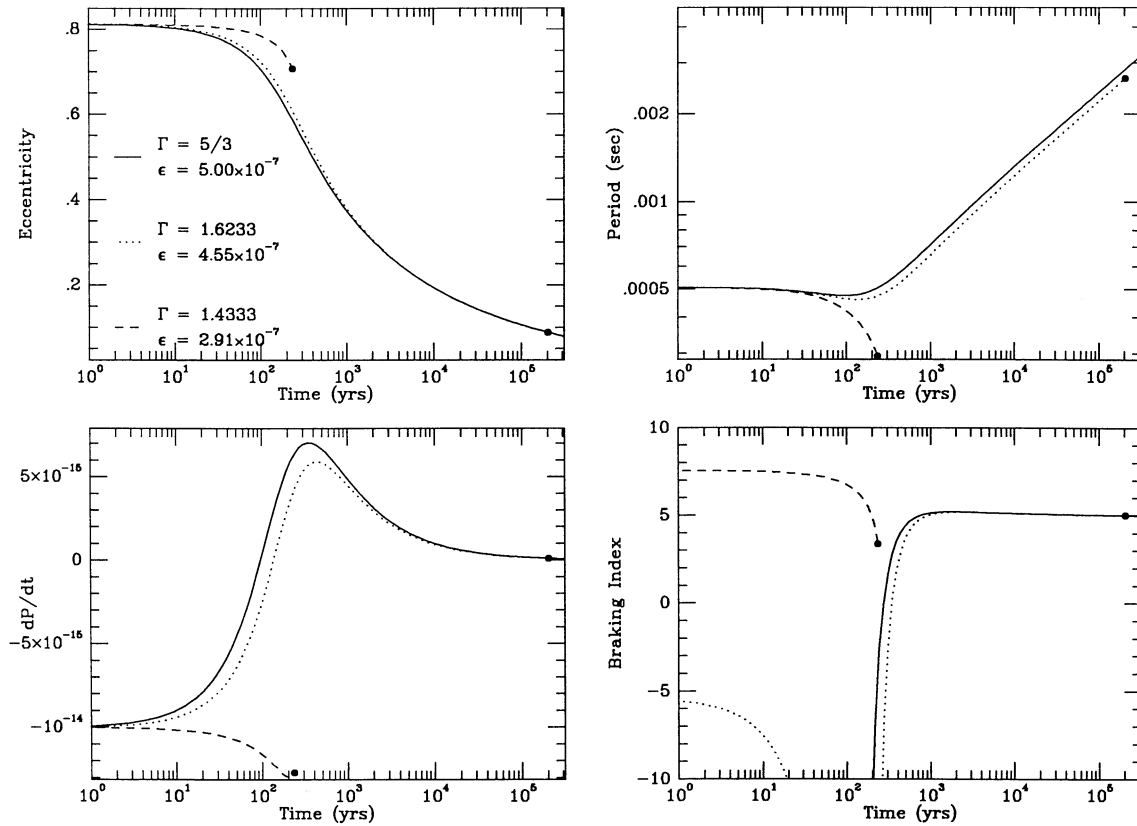


FIG. 5.—Spin evolution, via both gravitational and electromagnetic radiation, of a compressible Maclaurin spheroid model of an 0.5 ms pulsar. The gravitational radiation is assumed to come from an ellipsoidal deformation of fractional amplitude ϵ , and, like the magnetic moment, is chosen to be the maximum allowed by the observations of the pulsar and the supernova remnant. The three curves shown here correspond to the same equations of state shown in Fig. 4. The observational constraint on \dot{P} forces a very small ϵ ; nevertheless, gravitational radiation can still significantly affect the rapidity of the pulsar's evolution.

where $a > b > c$ are the semiaxes of the ellipsoid, and the final approximate equality is for the limit of small ellipsoidal deformation. The above result for the wave amplitudes agrees with the original formula of Shapiro (1979) for homogeneous, triaxial ellipsoids.

It is convenient to express h_+ and h_x in terms of a characteristic radiation amplitude h which is independent of time and the observer's orientation angle:

$$h \equiv \frac{4\epsilon}{r} I\Omega^2, \quad (73a)$$

$$h_+ = h \frac{\cos^2 \theta + 1}{2} \cos [2(\phi - \Omega t)], \quad (73b)$$

$$h_x = -h \cos \theta \sin [2(\phi - \Omega t)]. \quad (73c)$$

In all our models of an 0.5 ms pulsar, we assume that $P = 0.5$ ms when $e = e_{\text{sec}}$, regardless of Γ or \mathcal{K} . In this case, the characteristic gravitational radiation strain at birth is independent of the equation of state:

$$h = (2.3 \times 10^{-25}) \left(\frac{\epsilon}{5 \times 10^{-7}} \right) \left(\frac{55 \text{ kpc}}{r} \right) \left(\frac{M}{1.7 M_\odot} \right)^{5/3} \left(\frac{0.5 \text{ ms}}{P} \right)^{2/3}. \quad (74)$$

This periodic strain h is observable with 90% confidence in a $\frac{1}{3}$ yr integration time using present-day bar detector technology, though no currently operating bar detector has the correct resonant frequency. Present-day laser interferometric detectors are just shy of the necessary sensitivity to detect this strain; however, it will be easily measurable with the proposed Caltech-MIT LIGO antenna system (cf. Thorne 1987, § 9.4.2b and Fig. 9.6, and also § 9.5.2d-e for bar detectors, § 9.5.3c, eq. [112] and Fig. 9.11, for present-day interferometric detectors, and § 9.5.3g for the proposed LIGO detector).

In Figure 6 we look more closely at our models of an 0.5 ms pulsar that end in gravitational collapse to a black hole. Each curve in Figure 6 shows, for a different ϵ (or, through eq. [74], present-day h), the time at which the hoop conjecture predicts black hole formation. Note that the contours in Figure 6 do not depend on \mathcal{K} . The key point of Figure 6 is that evidence of eventual gravitational collapse to a black hole following early detection of a fast pulsar would provide a stringent constraint on allowed

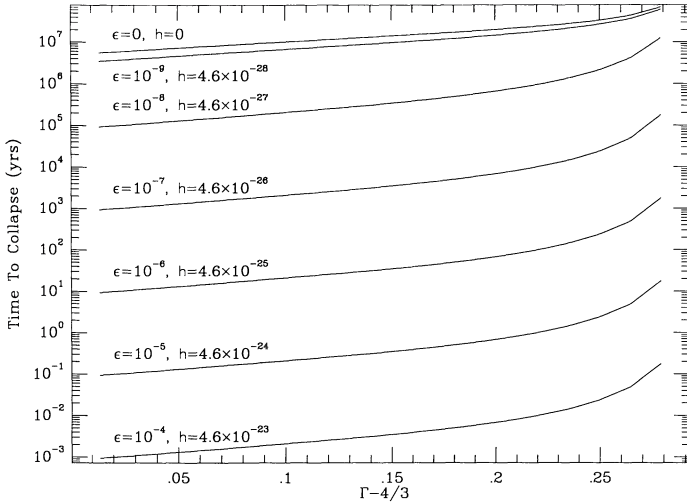


FIG. 6

FIG. 6.—Age of a fast pulsar, born with an 0.5 ms period, at gravitational collapse to a black hole for different degrees of triaxial deformation as a function of the adiabatic index. In our model, collapse to a black hole is inevitable for all equations of state whose adiabatic index satisfies $\Gamma - 4/3 < 0.2926$. Contours of fixed fractional ellipsoidal deformation and present-day gravitational radiation amplitude are shown.

FIG. 7.—Gravitational radiation luminosity of a test asymmetry on a rapidly rotating oblate spheroid relative to a spherical star. At zero angular momentum, both stars have the same mass and density. As the angular momentum is increased, the eccentricity of the oblate model is allowed to change while the spherical model is constrained to keep the same shape. The oblateness of a rapidly rotating star enhances the luminosity of a small mountain. Since softer equations of state lead to larger variations in the moment of inertia, the enhancement is greatest for the softest equations of state.

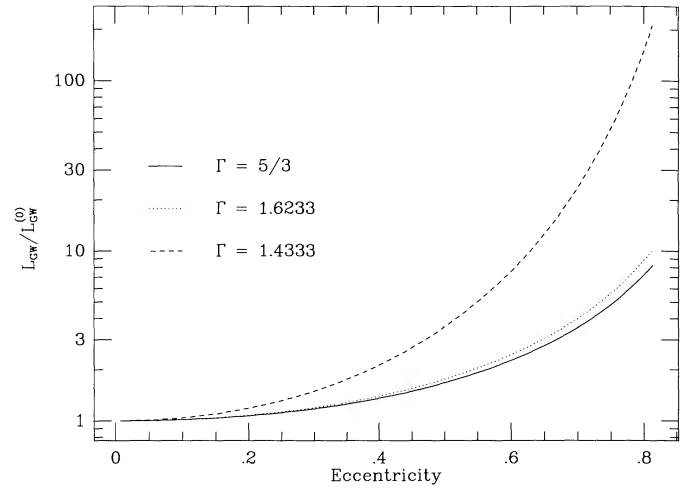


FIG. 7

equations of state. The inferred constraint would depend on the mountain height parameter, ϵ , which can be measured by a gravitational wave detector before the final collapse.

The gravitational radiation luminosity of our model of a fast pulsar is

$$L_{\text{GW}} = \frac{32}{5} I^2 \epsilon^2 \Omega^6$$

$$\simeq \frac{32}{5} I_0^2 \epsilon^2 \Omega^6 \left(\frac{\rho}{\rho_0} \right)^{-4/3} (1 - e^2)^{-2/3}. \quad (75)$$

It is instructive to identify

$$L_{\text{GW}}^{(0)} \equiv \frac{32}{5} I_0^2 \epsilon^2 \Omega^6 = \left(\frac{0.5 \text{ ms}}{P} \right)^6 \left(\frac{\epsilon}{5 \times 10^{-7}} \right)^2 \begin{cases} 2.2 \times 10^{42} \text{ ergs s}^{-1} & \text{for } \Gamma = 5/3, \\ 1.8 \times 10^{42} \text{ ergs s}^{-1} & \text{for } \Gamma = 1.6233, \\ 0.87 \times 10^{41} \text{ ergs s}^{-1} & \text{for } \Gamma = 1.4333, \end{cases} \quad (76)$$

which is the characteristic luminosity omitting the oblate distortion factors. Figure 7 shows how the oblateness distortion correction $L_{\text{GW}}/L_{\text{GW}}^{(0)}$ varies with e for the three values of Γ in Figures 4 and 5. It is immediately apparent that conventional estimates of the gravitational radiation from rapidly rotating pulsars omitting these factors may be vastly underestimated: *for large eccentricity the star's oblateness greatly enhances its wave luminosity*. Thus, even though the canonical ellipsoidal deformation is small ($\epsilon \lesssim 5 \times 10^{-7}$), the strain itself is relatively large (cf. eq. [74]). *Bearing this in mind, the detection of gravitational radiation from SN 1987A is particularly crucial if it never appears as a radio (or optical) pulsar.*

d) Flux Freezing

Up to now, all of our calculations have assumed that the projected magnetic dipole moment $\mu \sin \alpha$ is constant. As a spheroid spins down and its eccentricity changes, this condition leads to a changing magnetic flux through the surface. Here, for comparison, we consider models where the magnetic flux, and not the magnetic dipole moment, is held constant.

Suppose that, at some eccentricity e , the magnetic field exterior to a spheroid is an exact magnetic dipole and that the magnetic field lines are rigidly attached to its surface. As the eccentricity changes and each surface element is translated and deformed, the resulting magnetic field does *not* remain dipolar. The calculation of the new field is quite complicated and of limited value, since the other approximations that have gone into our model do not justify this level of precision. There is, however, an approximation that simplifies the calculation and is within the spirit of our spheroidal models.

First we introduce corotating body coordinates x , y , and z . The z -axis coincides with the symmetry (rotation) axis of the spheroid, and the magnetic dipole moment μ is the presumed to lie in the x - z plane so that it may be expressed as $\mu^z e_z + \mu^x e_x$. Our approximation is to assume that the two fluxes \mathcal{F}^x and \mathcal{F}^z through the open surfaces of the spheroid defined alternately by $x > 0$

and $z > 0$ are separately constant and that the field readjusts itself as the oblateness changes so that it always remains dipolar, with dipole moment in the x - z plane. This is sufficient to completely fix the magnetic dipole moment during the spin-down of the star.

To evaluate either \mathcal{F}^x and \mathcal{F}^z , we use Gauss's theorem on a closed surface that includes the relevant surface of the spheroid. For \mathcal{F}^z , the closed surface consists of the $z > 0$ surface of the spheroid, the $z > 0$ hemisphere at large radius \mathcal{R} , and the $z = 0$ annulus that closes the surface:

$$\mathcal{S}_a^z \equiv \{x, y, z: x^2 + y^2 + z^2/(1 - e^2) = a^2 \text{ and } z > 0\}, \quad (77a)$$

$$\mathcal{S}_0^z \equiv \{x, y, z: a^2 < x^2 + y^2 < \mathcal{R}^2 \text{ and } z = 0\}, \quad (77b)$$

$$\mathcal{S}_{\mathcal{R}}^z \equiv \{x, y, z: x^2 + y^2 + z^2 = \mathcal{R}^2 \text{ and } z > 0\}. \quad (77c)$$

The flux \mathcal{F}^x is evaluated using the closed surface consisting of the $x > 0$ surface of the spheroid, a *self-similar* surface at large radius \mathcal{R} , and the *elliptical* annulus that closes the surface:

$$\mathcal{S}_a^x \equiv \{x, y, z: x^2 + y^2 + z^2/(1 - e^2) = a^2 \text{ and } x > 0\}, \quad (78a)$$

$$\mathcal{S}_0^x \equiv \{x, y, z: a^2 < y^2 + z^2/(1 - e^2) < \mathcal{R}^2 \text{ and } x = 0\}, \quad (78b)$$

$$\mathcal{S}_{\mathcal{R}}^x \equiv \{x, y, z: x^2 + y^2 + z^2/(1 - e^2) = \mathcal{R}^2 \text{ and } x > 0\}. \quad (78c)$$

The total flux through either of these closed surfaces ($\mathcal{S}_0 + \mathcal{S}_a + \mathcal{S}_{\mathcal{R}}$) vanishes ($\nabla \cdot \mathbf{B} = 0$). Noting that

$$\mathbf{B} \equiv \frac{3\hat{\mathbf{n}}(\mathbf{n} \cdot \boldsymbol{\mu}) - \boldsymbol{\mu}}{r^3} \quad (79)$$

where $\hat{\mathbf{n}}$ is the unit direction vector, the flux through either $\mathcal{S}_{\mathcal{R}}^x$ or $\mathcal{S}_{\mathcal{R}}^z$ vanishes as $\mathcal{R} \rightarrow \infty$. Consequently, either of the fluxes \mathcal{F}^x or \mathcal{F}^z is the opposite of the flux through the corresponding annular surfaces \mathcal{S}_0^x or \mathcal{S}_0^z . These fluxes are simple to compute, and we find

$$\mathcal{F}^x = \frac{\mu^x}{a} \frac{4E(e)}{(1 - e^2)^{1/2}}, \quad (80a)$$

$$\mathcal{F}^z = \frac{2\pi\mu^z}{a}, \quad (80b)$$

where $E(e)$ is the complete elliptic integral of the second kind:

$$E(e) \equiv \int_0^{\pi/2} d\phi (1 - e^2 \sin^2 \phi)^{1/2}. \quad (81)$$

Our condition on $\boldsymbol{\mu}$ is that \mathcal{F}^x and \mathcal{F}^z be separately constant, or

$$\left(\frac{\mu^x}{\mu_0^x}\right) = \frac{\pi}{2} \frac{(1 - e^2)^{1/3}}{E(e)} \left(\frac{\rho}{\rho_0}\right)^{-1/3}, \quad (82a)$$

$$\left(\frac{\mu^z}{\mu_0^z}\right) = (1 - e^2)^{-1/6} \left(\frac{\rho}{\rho_0}\right)^{-1/3}, \quad (82b)$$

where μ_0^x and μ_0^z are the components of the dipole moment at zero eccentricity. Only $\mu^x = \mu \sin \alpha$ is important for the radiative loss of angular momentum.

In Figure 8 we repeat the calculation shown in Figure 4 of the electromagnetic spin-down of an 0.5 ms pulsar, only now with a flux-frozen magnetic field instead of a constant magnetic dipole moment. For this calculation we take the initial projected moment $\mu^x(e_{\text{sec}})$ to be $4.2 \times 10^{26} \text{ G cm}^3$ (which is the value of the constant magnetic dipole moment assumed in the earlier calculation). The magnetic dipole moment sets the time scale for the evolution of the models, and its effects are most clearly seen in \dot{P} and the braking index. Also shown is the variation in μ^x as the star evolves. The effect of flux freezing is to slow the evolution of the pulsar: as the neutron star spins down, the projected magnetic dipole moment is reduced and with it the rate of energy and angular momentum loss. This is important in rapidly rotating pulsars where the eccentricity is large; however, when e becomes small, the magnetic dipole moment becomes constant and flux freezing is unimportant to the calculation.

IV. ACCRETION

Here we briefly renew our discussion of accretion deferred from §§ II and III. We focus on accretion from an aligned Keplerian disk in the equatorial plane of an oblate Maclaurin spheroid. We assume that accretion takes place at the inner edge $r_0 > a$ of the disk, with the deposited angular momentum being that of the gas in a circular orbit at r_0 . Then

$$\mathbf{J} = \dot{M} \Omega_{\mathbf{k}}(r_0) r_0^2 = \dot{M} \Omega a^2 \left[\frac{\Omega_{\mathbf{k}}}{\Omega} \frac{r_0^2}{a^2} \right]. \quad (83)$$

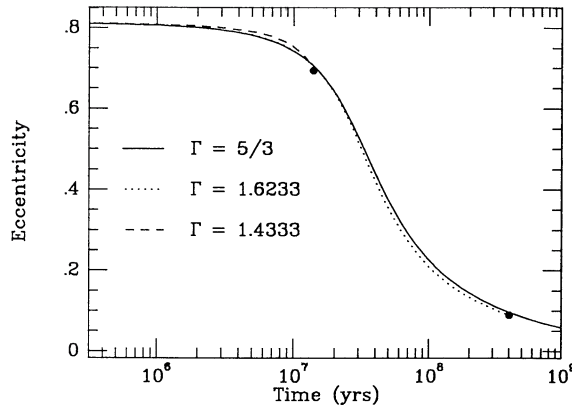


FIG. 8a

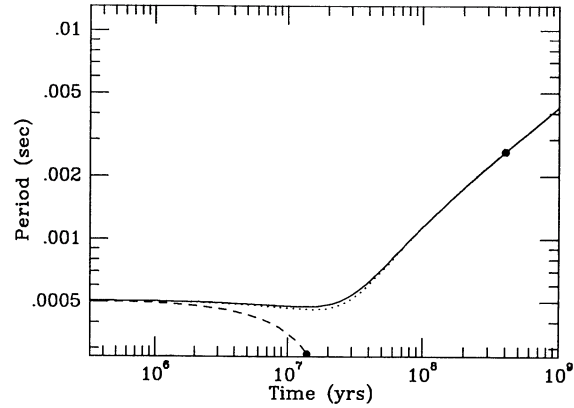


FIG. 8b

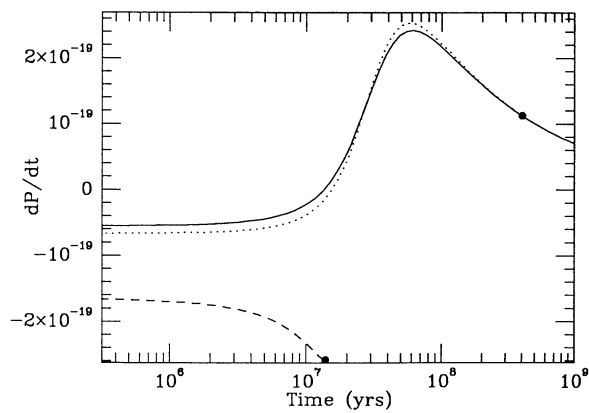


FIG. 8c

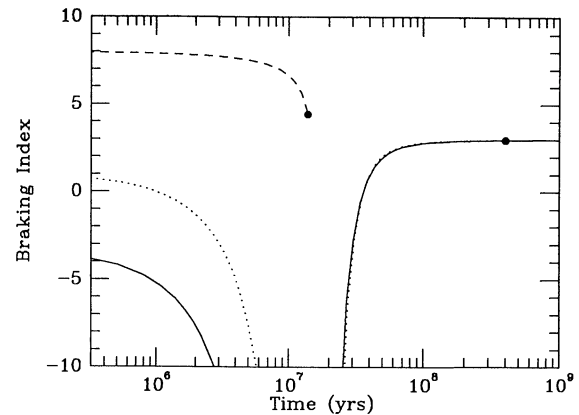


FIG. 8d

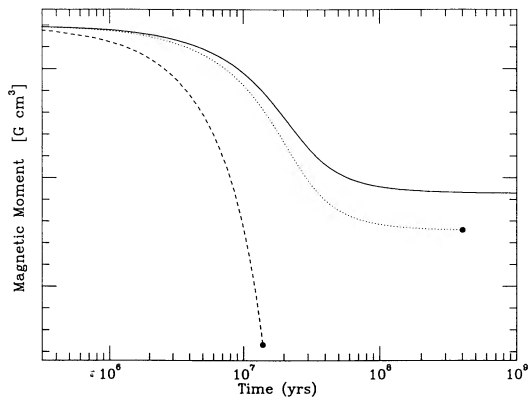


FIG. 8e

FIG. 8.—If the magnetic flux through the surface of a pulsar is held constant, the magnetic dipole moment changes as the eccentricity changes, and this changes the time scale for spin-down from rapid rotation. Here we show the spin evolution of a pulsar born with a period of 0.5 ms via magnetic dipole radiation, modeled as a sequence of *compressible* Maclaurin spheroids. In contrast to Fig. 4, however, we assume here that the magnetic flux is frozen into the star's surface (see the text). Panel e shows how the projected magnetic dipole moment $\mu \sin \alpha$ changes with time.

It is useful (Ghosh and Lamb 1978) to identify a “fastness parameter” ω_s which indicates how close the equatorial velocity of the spheroid is to the Keplerian velocity at the accretion radius:

$$\omega_s^2 \equiv \frac{\Omega^2}{\Omega_K^2}. \quad (84)$$

We also identify the bracketed term in equation (83) by f :

$$f \equiv \left[\frac{1}{\omega_s} \frac{r_0^2}{a^2} \right]. \quad (85)$$

For disk accretion induced by magnetic drag onto a magnetized neutron star, we expect that the accretion radius r_0 is approximately half the Alfvén radius r_A (boundary of the magnetosphere; Ghosh and Lamb 1978). To maintain a steady state accretion and

avoid the “propeller” effect at this radius, the fastness parameter must be less than unity; hence, $f > 1$ (cf. ST, Chap. 15 and references therein for further discussion). In applying equation (83), we are neglecting viscous and magnetic torques acting on the star-plus-magnetosphere, which may be important for “fast rotators” with large ω_s .

To determine Ω_K for a homogeneous spheroid, note that in the equatorial plane the gravitational force is

$$F(r) = -\frac{3}{2} \frac{M}{r^2} \eta^{-3} [\sin^{-1} \eta - \eta(1 - \eta^2)^{1/2}] e, \quad (86)$$

where $\eta \equiv ae/r$ (Mihalas and Routly 1986). Consequently,

$$\Omega_K^2(r_0) = \frac{F(r_0)}{r_0} = \frac{3}{2} \frac{M}{r_0^3} \eta^{-3} [\sin^{-1} \eta - \eta(1 - \eta^2)^{1/2}] \quad (87)$$

and

$$f = \left[\frac{g(e)}{(1 - e^2)^{1/2} e} \right]^{-1/2} \eta^{-2} [\sin^{-1} \eta - \eta(1 - \eta^2)^{1/2}]^{1/2}. \quad (88)$$

In the absence of electromagnetic and gravitational torques, equation (47) becomes

$$\frac{dM}{dt} \Omega a^2 \left(f - \frac{2}{5} \frac{5\Gamma - 7}{3\Gamma - 4} \right) = \frac{1}{2} I \Omega \left[\frac{g'}{g} + \frac{1}{3\Gamma - 4} \left(\frac{4(\Gamma - 1)e}{1 - e^2} - \frac{A'_3}{A_3} \right) \right] \frac{de}{dt}. \quad (89)$$

This equation encompasses both the compressible models discussed in § III and the incompressible models discussed in § II (which correspond to the limit $\Gamma \rightarrow \infty$).

Consider, for definiteness, the incompressible models, for which equation (89) may be reexpressed as

$$\frac{dM}{dt} \Omega a^2 \left(f - \frac{2}{3} \right) = \frac{1}{2} I \Omega \left[\frac{g'}{g} = \frac{4}{3} \frac{e}{1 - e^2} \right] \frac{de}{dt} \quad (90)$$

$$= I \Omega \left[1 + \frac{4}{3} \frac{g}{g'} \frac{e}{1 - e^2} \right]. \quad (91)$$

The expression in brackets multiplying $\dot{\Omega}$ is positive $e < e_{\text{sec}}$; consequently, for incompressible models, accretion spin-up versus spin-down is determined by the sign of $(f - \frac{2}{3})$: positive for spin-up and negative for spin-down. Thus, for steady disk accretion onto a magnetized neutron star where $f > 1$, we always expect spin-up in the absence of magnetic torques.

The alternative special case of unsteady accretion with vanishing $\dot{\Omega}$, which corresponds to $f = \frac{2}{3}$, or

$$\frac{9}{4} \eta^{-4} [\sin^{-1} \eta - \eta(1 - \eta^2)^{1/2}] = \frac{g(e)}{e(1 - e^2)^{1/2}} \quad (92)$$

for $\eta < e < e_{\text{sec}}$, is impossible in this model. Equation (92) has no solution for $0 < e < e_{\text{sec}}$, so for these self-consistent models accretion from an aligned disk only leads to spin-up. For the compressible models the situation is more complicated. The evolution of eccentricity is described by equation (89), so accretion that does not change the star's eccentricity requires

$$\eta^{-2} [\sin^{-1} \eta - \eta(1 - \eta^2)^{1/2}]^{1/2} = \frac{2}{5} \frac{5\Gamma - 7}{3\Gamma - 4} \left[\frac{g(e)}{(1 - e^2)^{1/2} e} \right]^{1/2}. \quad (93)$$

In the domain $\Gamma \in (\infty, 4/3)$, this equation also has no roots, and so accretion from an aligned disk always increases the eccentricity of the star. However, as we saw in § III, Ω is *not* monotonic in e for rapidly rotating stars, and so accretion can lead to spin-down even as the angular momentum increases. For reference, the relationship between \dot{M} and $\dot{\Omega}$ for the accretion discussed here is

$$\begin{aligned} \Omega a^2 \frac{dM}{dt} \left(f - \frac{2}{15} \left[5 - \frac{4}{3\Gamma - 4} \left\{ 1 + \frac{1}{\Gamma - 4/3} \left(\frac{\Gamma e}{1 - e^2} - \frac{A'_3}{A_3} \right) \left[\frac{g'}{g} + \frac{1}{\Gamma - 4/3} \left(\frac{A'_3}{A_3} - \frac{4}{3} \frac{e}{1 - e^2} \right) \right]^{-1} \right\} \right] \right) \\ = I \Omega \left\{ 1 + \frac{4/3}{\Gamma - 4/3} \left(\frac{\Gamma e}{1 - e^2} - \frac{A'_3}{A_3} \right) \left[\frac{g'}{g} + \frac{1}{\Gamma - 4/3} \left(\frac{A'_3}{A_3} - \frac{4}{3} \frac{e}{1 - e^2} \right) \right]^{-1} \right\}. \quad (94) \end{aligned}$$

V. CONCLUSIONS

We have used exact compressible and incompressible sequences of Maclaurin spheroids to model the evolution of rapidly rotating pulsars by accretion, electromagnetic radiation, and gravitational radiation. Using the hoop conjecture (Thorne 1972), we have explored the formation of black holes by the loss of rotational support during pulsar spin-down.

We have found that a rapidly rotating pulsar's changing oblateness has observable consequences in measurements of its \dot{P} and braking index. During spin-down from rapid rotation, the star's decreasing oblateness reduces its moment of inertia. For very stiff equations of state, this suppresses \dot{P} somewhat at high rotation rates, but for softer equations of state \dot{P} can actually be *negative*,

corresponding to spin-up, even as the pulsar is losing angular momentum. (At slower rotation rates, the star is spherical, the moment of inertia constant, and \dot{P} is proportional to \dot{J} .)

Two examples are used to illustrate the usefulness of these exact models: a rapidly rotating pulsar born with an 0.5 ms period, and the Crab pulsar.

In modeling the 0.5 ms pulsar, the results of Friedman, Ipser, and Parker (1989) suggest that the mass of the pulsar is greater than $1.7 M_{\odot}$. We show in a self-consistent calculation that for this mass almost all equations of state softer than that of an ideal nonrelativistic Fermi neutron gas lead to the eventual gravitational collapse of the pulsar and the formation of a black hole following loss of rotational energy and angular momentum. The age of the pulsar when it collapses depends sensitively on the equation of state and the strength of the gravitational quadrupole and magnetic dipole radiation from the star.

We have also reexamined the Ostriker and Gunn (1969) calculation of the age of the Crab pulsar. While the Crab is not now spinning rapidly, the original calculation of its spin evolution suggested that it was spinning rapidly at birth. Not surprisingly, we found that its oblateness at early ($e \gtrsim 0.3$) times would have had observable consequences in the first several years following its birth.

In our simple homogeneous, uniformly rotating Newtonian models, the oblateness of rapidly rotating stars increases the efficiency of gravitational radiation well over what one would estimate without taking the rotational deformation into account. When we adopt even a very modest $\sim 5 \times 10^{-7}$ (which is consistent with current theoretical suggestions), *the amplitude of the gravitational radiation is large enough to be detectable at the 90% confidence level with a 3 month integration time using present-day bar detector technology.*

Our models also suggest how \dot{P} and the braking index of rapidly rotating pulsars can be used to probe the star's structure and equation of state.

While the models explored here are all Newtonian, relativistic generalizations of Maclaurin spheroids have been constructed (Butterworth and Ipser 1976). Most of the conclusions we have reached are independent of the detailed rate of angular momentum transport and depend only on the fact that the moment of inertia of a rapidly rotating star changes with its angular velocity. Accordingly, we expect that a similar analysis of homogeneous relativistic spheroids is possible and would yield similar results. Moreover, the same qualitative conclusions should apply to inhomogeneous equilibrium stars (Newtonian or relativistic) but are less dramatic, the more centrally condensed the configurations.

We would like to thank Ira Wasserman and David Chernoff for stimulating and helpful discussions, and Gerald Quinlan for assistance with the algebraic manipulator Maple. This work was supported by National Science Foundation grants PHY 86-03284 and AST 87-14475 to Cornell University. Some of the computations in support of this research were carried out at the Cornell National Supercomputing Facility, which is supported in part by the National Science Foundation, IBM Corporation, New York State, and the Cornell Research Institute. S. L. S. also gratefully acknowledges fellowship support from the John Simon Guggenheim Memorial Foundation.

REFERENCES

- Alpar, M. A., and Pines, D. 1985, *Nature*, **314**, 334.
 Arons, J. 1983, *Nature*, **302**, 301.
 Brecher, K., and Channugam, G. 1978, *Ap. J.*, **221**, 969.
 ———. 1983, *Nature*, **302**, 124.
 Butterworth, E. M., and Ipser, J. R. 1976, *Ap. J.*, **204**, 200.
 Chandrasekhar, S. 1986, *Ellipsoidal Figures of Equilibrium* (New York: Dover).
 Cowsik, R., Ghosh, P., and Melvin, M. A. 1983, *Ap. J.*, **303**, 308.
 Friedman, J. L., Ipser, J. R., and Parker, L. 1986, *Ap. J.*, **304**, 115.
 ———. 1989, preprint.
 Ghosh, P., and Lamb, F. K. 1978, *Ap. J. (Letters)*, **223**, L83.
 Hartle, J. B. 1970, *Ap. J.*, **161**, 111.
 Kochanek, C. S., Shapiro, S. L., Teukolsky, S. A., and Chernoff, D. F. 1990, *Ap. J.*, in press.
 Kristian, J., et al. 1989, *Nature*, **338**, 234.
 Middleditch, J. 1989, preprint.
 ———. 1990, reported at AAAS Meeting New Orleans, 1990.
 Mihalas, D., and Routly, P. M. 1968, *Galactic Astronomy* (San Francisco: Freeman).
 Misner, C. W., Thorne, K. S., and Wheeler, J. A. 1973, *Gravitation* (San Francisco: Freeman).
 Ostriker, J. P., and Gunn, J. E. 1969, *Ap. J.*, **157**, 1395 (OG).
 Pines, D., and Shaham, J. 1972, *Nature Phys. Sci.*, **235**, 43.
 Shapiro, S. L. 1979, in *Sources of Gravitational Radiation*, ed. L. Smarr (Cambridge: Cambridge University Press).
 Shapiro, S. L., and Teukolsky, S. A. 1983, *Black Holes, White Dwarfs, and Neutron Stars* (New York: Wiley) (ST).
 Shapiro, S. L., Teukolsky, S. A., and Wasserman, I. 1983, *Ap. J.*, **272**, 702.
 ———. 1989, *Nature*, **340**, 451.
 Sorrell, W. H. 1989, preprint.
 Thorne, K. S. 1972, in *Magic without Magic: John Archibald Wheeler*, ed. J. Klauder (San Francisco: Freeman).
 ———. 1987, in *300 Years of Gravitation*, ed. S. Hawking and W. Israel (Cambridge: Cambridge University Press), p. 330.
 Woosley, S. E., and Chevalier, R. A. 1989, *Nature*, **338**, 321.

LEE S. FINN and STUART L. SHAPIRO: Space Sciences Building, Cornell University, Ithaca, NY 14853